Interaction of *Chlorella vulgaris*: Cell Attachment on Nanocellulose-Based Hydrogel for Sustainable Microalgae Cultivation

Wan Nazihah Liyana Wan Jusoh [a,b] Mohd Shaiful Sajab [a,b,*] Nazlina Haiza Mohd Yasin [c] Peer Mohamed Abdul [a,b] and Mohd Sobri Takriff [d,a,b]

** Corresponding author: mohdshaiful@ukm.edu.my*

DOI: 10.15376/biores.20.1.201-218

GRAPHICAL ABSTRACT

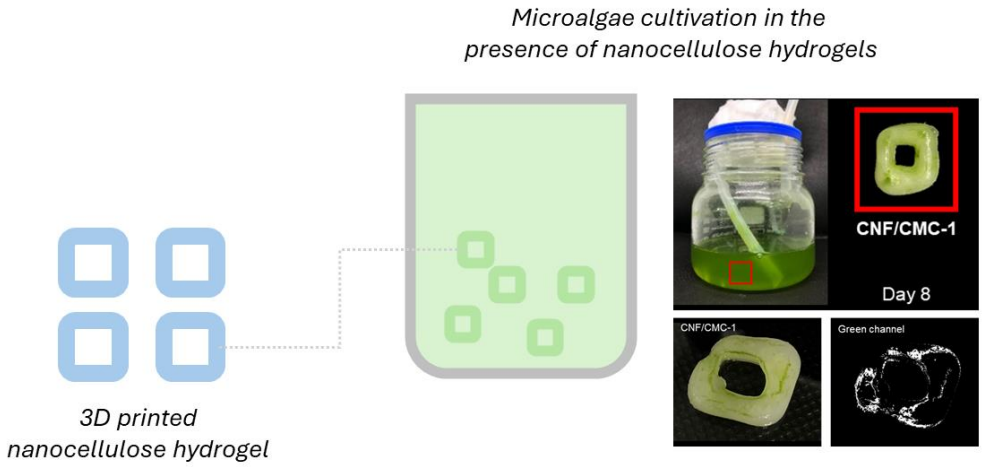

Microalgae cell attachment on nanocellulose based hydrogel

Interaction of *Chlorella vulgaris*: Cell Attachment on Nanocellulose-Based Hydrogel for Sustainable Microalgae Cultivation

Wan Nazihah Liyana Wan Jusoh [a,b] Mohd Shaiful Sajab [a,b,*] Nazlina Haiza Mohd Yasin [c] Peer Mohamed Abdul [a,b] and Mohd Sobri Takriff [d,a,b]

This study explores the potential of nanocellulose-based hydrogel for microalgae cell attachment. The hydrogel, composed of cellulose nanofibrils (CNF) and carboxymethyl cellulose (CMC), indicates feasibility in biomedical and cell culturing applications. It qualifies as an excellent substrate for 3D printing bioink utilizing the liquid deposition modelling technique. The growth of *Chlorella vulgaris* cells in Bold Basal Media (BBM) solution exhibits similar trends for both the standard culture and the culture media incorporating the CNF/CMC hydrogel. It was observed that the ionic-bond crosslinkers of H_2SO_4 and $CaCl_2$ in hydrogel formation were more conducive to cell adhesion compared to using covalent-bond crosslinkers of epichlorohydrin. Microalgae cell attachment exhibited the increase of green hue on the hydrogel surfaces, which shows the potential of cell to grow in the presence of CNF/CMC hydrogel.

DOI: 10.15376/biores.20.1.201-218

Keywords: Adhesion; Cellulose; Crosslinker; Chlorella vulgaris; Hydrogel

Contact information: a: Research Center for Sustainable Process Technology (CESPRO), Faculty of Engineering and Built Environment, Universiti Kebangsaan Malaysia, 43600 Bangi, Selangor, Malaysia; b: Department of Chemical and Process Engineering, Faculty of Engineering and Built Environment, Universiti Kebangsaan Malaysia, 43600 Bangi, Selangor, Malaysia; c: Department of Biological Sciences and Biotechnology, Faculty of Science and Technology, Universiti Kebangsaan Malaysia, 43600, UKM, Bangi, Selangor, Malaysia; d: Department of Mechanical and Nuclear Engineering, College of Engineering, University of Sharjah, United Arab Emirates;
**Corresponding author: mohdshaiful@ukm.edu.my*

INTRODUCTION

Biomaterials have emerged as a prominent field of study in recent years because of their unique properties and wide-ranging applications. These materials can exist in both active and passive states, and they can be either naturally derived or biologically produced (Troy *et al.* 2021; Liu *et al.* 2023). Their remarkable compatibility with living organisms and biological systems has led to their extensive use in the biomedical field, particularly in tissue engineering and drug delivery (Langer 2000; Jusoh *et al*. 2022; Liu *et al.* 2022). Alongside the growing interest in biomaterials, hydrogels, a soft material with high water content that mimics the extracellular matrix, have also gained significant attention (González-Díaz and Varghese 2016; Norioka *et al.* 2021). Hydrogels find applications in diverse areas such as biomedical, agricultural, sensor technology, and ecological preservation (Pyarasani *et al.* 2018; Correa *et al.* 2021).

Cellulose-based hydrogel, a groundbreaking addition to the hydrogel family, is derived from cellulose and its derivatives. It is produced from local resources rich in

cellulose such as kenaf, cotton, oil palm, microalgae, and bacteria (Hua *et al*. 2020; Naomi *et al.* 2020; Chopra and Manikanika 2022; Yap *et al.* 2023). Despite solubility and hydrophilicity challenges (Ciolacu *et al.* 2020; Zou *et al.* 2022), these hydrogels are gaining attention due to their excellent properties such as high mechanical strength, biocompatibility, quick degradation rate, and the fact that they are safe (Kabir *et al.* 2018; Cui *et al.* 2019; Zainal *et al.* 2021; Ban *et al.* 2022; Chen *et al.* 2022). The application of hydrogel is intrinsically linked to biological entities and living cells, which necessitate a high-water content, biocompatible material with minimal toxicity (Mantha *et al.* 2019; Dattilo *et al.* 2023). Some studies have been conducted to understand the interaction of cellulose with living cells. Even though the attachment of living cells on the cellulose plant cell wall may not be optimal, it facilitates cell-to-cell interaction, supports bacterial attachment, and aids bacterial tolerance (Jusoh *et al*. 2022).

The viability and growth potential of cells can be assessed through their attachment to the hydrogel surfaces, which also provides insights into the toxicity of the hydrogel. Cell growth is environment-dependent and cannot thrive in harsh and highly toxic conditions. Several studies have explored cell attachment potential on cellulose hydrogels from various sources such as birch kraft pulp, diethylaminoethyl cellulose, seaweed, *nata de coco*, and *Acetobacter* culture (Tan *et al.* 2016; Johns *et al.* 2018; Loh *et al.* 2018; Pajorova *et al.* 2020; Bar-Shai *et al.* 2021; Vel *et al.* 2022). Bacterial cellulose hydrogel demonstrates effective cell attachment, viability, and cell transfer for keratinocytes and fibroblasts, making them suitable for wound healing applications. The hydrophilic nature of hydrogel enhances cell attachment (Loh *et al.* 2018). Meanwhile, for the growth and attachment of marine macroalgae, the prepared scaffolds were found to exhibit high topographical cues affecting cell attachment and interaction, thus demonstrating non-toxic properties with increased cell viability using fibroblasts (Bar-Shai *et al.* 2021).

Despite numerous studies focusing on the interaction of hydrogel with cells, there are still gaps in understanding the prospects involving cellulose-based hydrogel especially the exploration of cell attachment using cellulose, those derived from oil palm biomass. The conditions for growth and the survival ability of cells with the cellulose-based hydrogel are yet to be identified. Therefore, this work aims to understand the potential of cellulose-based hydrogel in providing a conducive environment for cell growth and promoting the attachment of microalgae cells, specifically *Chlorella vulgaris*. The oil palm biomass was chosen as the raw material for hydrogel fabrication due to its strength, low cost, and high availability. The *C. vulgaris* is cultured and grows in conjunction with the cellulose-based hydrogel for eight days, and the optical density (OD) of the media and color effect of the hydrogel is recorded. The impact of hydrogel crosslinkers of ionic-bond, (H_2SO_4 and $CaCl_2$) and covalent-bond (epichlorohydrin (ECH)) on microalgae attachment is also examined. It was discovered that the growth of microalgal cells within encapsulated hydrogel promoted the growth duration due to easy access and high circulation of nutrients.

EXPERIMENTAL

Materials

Cellulose was extracted from the raw material, oil palm empty fruit bunch (OPEFB) fiber, which ranges in size from 106 to 500 µm. The preparation of cellulose and cellulose ink involved the use of 90% formic acid, 30% hydrogen peroxide (H_2O_2), iron (0) sourced from iron (II) sulfate heptahydrate ($Fe_2SO_4{\cdot}7H_2O$), lithium hydroxide, urea, sodium

carboxymethyl cellulose, sulfuric acid (H_2SO_4), and calcium chloride ($CaCl_2$), all obtained from Merck, Darmstadt, Germany. The Bold Basal Medium are the combination of macronutrient, alkaline ethylenediaminetetraacetic acid (EDTA) solution, acid iron solution, boron solution, and trace metal solution by following the previous study (Anderson 2005).

Preparation of Nanocellulose-based Hydrogel

The fractionation of cellulose and lignin from oil palm empty fruit bunch (OPEFB) fibers was conducted using an organosolv extraction process, as established in previous studies (Sajab *et al.* 2019; Mohan *et al.* 2021). Initially, lignin was extracted from OPEFB using 90% formic acid in a three-neck flask equipped with a condenser. The extraction was performed at a 30:1 ratio for 2 h at 90 °C. Excess organosolv lignin was filtered through a vacuum filter, and the pretreated pulp was washed with deionized water. To purify the cellulose from the pretreated pulp, undissolved lignin and hemicellulose were removed by catalytic oxidation using 5% w/v of 30% hydrogen peroxide and 10 mg/L of Fe(II) at 90 °C for 24 h. The purified cellulose pulp was then separated and thoroughly washed with deionized water until it appeared white.

Defibrillation of cellulose was achieved through mechanical shearing using a high-speed homogenizer (IKA T25 Digital, Staufen, IKA Germany). A 0.7 wt% cellulose suspension was fibrillated at 25,000 rpm in controlled cycles for a total of 30 min, ensuring the system temperature remained below 70 °C to prevent thermal hydrolysis of cellulose. For the preparation of CMC ink solution, 4.5 wt% of CMC was mixed with deionized water at 40 °C and stirred until fully dissolved. The prepared solutions of CNF and CMC were then vigorously stirred using a high-speed homogenizer (IKA T25 Digital, Staufen, IKA Germany) at 5,000 rpm for 10 min until a complete solution and thorough mixing were achieved.

Nanocellulose-based Hydrogel Formation

A liquid deposition modeling (LDM) was selected for 3D printing of cellulose-based hydrogel at various concentrations, given its aptitude for extruding ink from the liquid phase. The paste extruder (Structur3d Printing in Kitchener, Canada) was integrated with commercial 3D printer (Ultimaker 2+, Ultimaker, Geldermalsen, Netherlands). The design was created using computer-aided design (CAD) and sliced with Ultimaker Cura 4.5 (Ultimaker, Geldermalsen, Netherlands) following to the Discovery configuration. All printings were conducted using a nozzle with a diameter of 0.84 mm.

In the formation of hydrogel, two types of crosslinkers were utilized: 3% H_2SO_4 and $CaCl_2$, and epichlorohydrin (ECH). For the regeneration process using 3% H_2SO_4 and $CaCl_2$, the 3D-printed material was immersed in H_2SO_4 for several hours, followed by $CaCl_2$. Concurrently, the ECH was combined with the CNF/CMC solution prior to the printing process at the volume of 5% from the total solution. After the printing was completed, the 3D-printed material was left to dry at room temperature until it was completely dry. All the 3D materials were rinsed with distilled water before being used in subsequent experiments.

Preparation of *C. vulgaris* Inoculum

Bold's Basal Medium, the nutrient source for *C. vulgaris* cells, was prepared as per a previous study (Anderson 2005). All materials and tools were sterilized using an autoclave at 121 °C for 15 min. Subsequently, 10% of the *C. vulgaris* stock culture was

added to the 1.0 L sterilized BBM. The cells in this inoculum were allowed to grow under white light and aeration using air pump. Cell growth using the OD value is fitted into a kinetic model equation, which applies the cell mitosis approach and cell agglomeration method (Beruto *et al.* 2014; Paladino and Neviani 2020).

In the microalgal cell attachment study, the 3D-printed nanocellulose-based hydrogel was immersed in the microalgal culture, following the details outlined in Table 1 for different crosslinkers and culture conditions. The experiment was carried out over eight days at room temperature. For microalgal culture conditions in the BBM medium, it was conducted under two different media conditions: new culture and media with an OD of 0.8. However, for encapsulation conditions, the experiment was performed only in the new culture. This condition was applied for both types of crosslinkers. The OD of the culture and the image of the 3D-printed nanocellulose-based hydrogel were recorded daily.

Table 1. Formulation of 3D-printed Nanocellulose-based Hydrogel and Microalgae Culture Condition

Sample ID	Hydrogel Composition (CNF:CMC:BBM)	Crosslinker	*C. vulgaris* Culture Condition
CNF-1	1:0:0	H_2SO_4	BBM medium
CNF-2	1:0:0	ECH	BBM medium
CNF/CMC-1	1:1:0	H_2SO_4 + $CaCl_2$	BBM medium
CNF/CMC-2	1:1:0	ECH	BBM medium
CNF/CMC/BBM-1	1:1:1	H_2SO_4 + $CaCl_2$	BBM medium
CNF/CMC/BBM/E-1	1:1:1	H_2SO_4 + $CaCl_2$	Encapsulation
CNF/CMC/BBM-2	1:1:1	ECH	BBM medium
CNF/CMC/BBM/E-2	1:1:1	ECH	Encapsulation

Characterization

The OD of the culture media was analysed using a spectrophotometer (DR1900, HACH, Loveland, CO, USA) at the wavelength of 750 nm and the color changes by a digital camera (Griffiths *et al.* 2011; Scarponi *et al.* 2021). The structures of microalgae and CNF/CMC hydrogel were examined using optical microscope (B-380 series, OPTIKA microscope, Bergamo, Italy) and a field emission scanning electron microscope (FESEM) (Merlin Compact, Zeiss Pvt Ltd, Oberkochen, Germany). Prior to analysis, the samples were placed on an aluminium mount and coated with iridium using a sputter coater to avoid electrical charging. A computer aided imaging analysis is conducted by using open source, Fiji software (https://imagej.net/software/fiji/), with the incorporation of processing package, ImageJ (Version 2.15.1) for quantitative analysis of the cell growth. ImageJ is the image processing software commonly used for visualizing, validating, and quantifying the image data into more understandable form according to the experimental needs. The image and color of the CNF/CMC hydrogel and microalgal cells were identified and classified based on their color and tones (Carbone *et al.* 2017). The color channel is set depends on the desired color analysis and is presented in the black and white image.

RESULTS AND DISCUSSION

CNF/CMC Hydrogel

The extracted CNF and hydrogel CNF/CMC were characterized by morphology to understand the biomaterial structure. Figure 1(a) shows the CNF micrograph in which the

structure was more dispersed and formed fibrils like a spider web (Sajab *et al*. 2019). The observed size of the CNF fibrils was smaller compared to cellulose, showing that the size reduction occurred during the mechanical disintegration process. The production of CNF was also evidenced by the TEM analysis with the observed size in between 15 and 50 nm, which is also supported by previous study (Kargarzadeh *et al*. 2018). The SEM image of CNF/CMC hydrogel is shown in Fig. 1(c) after the regeneration process. High porosity structure of hydrogel can be seen clearly in Fig. 1(d) from TEM analysis. The increase of pores in the hydrogel will help for a better absorption and attachment based on higher surface area available (Annabi *et al*. 2010).

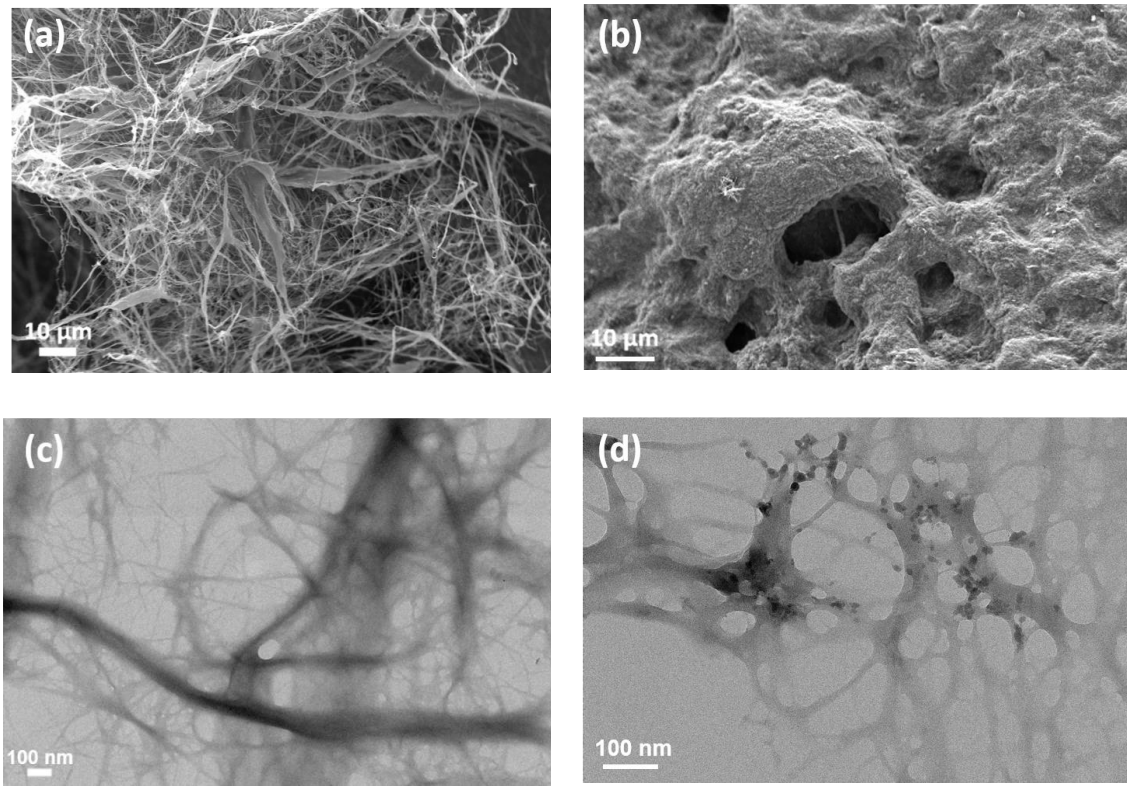

Fig. 1. Morphology analysis after cellulose extraction (a) CNF (SEM); (b) CNF/CMC (SEM); (c) CNF (TEM); (d) CNF/CMC (TEM).

In this study, all formulated hydrogels were 3D printed with a simple structure. A square shape with a central hole, measuring 15 × 15 mm^2, was selected for the cell adhesion experiment. Figure 2 depicts the 3D-printed nanocellulose-based hydrogel prior to the crosslinking process. The 3D-printed nanocellulose-based hydrogel post-crosslinking, using two types of crosslinkers: ionic-bonded (H_2SO_4 and $CaCl_2$) and covalent-bonded (ECH) crosslinkers. The H_2SO_4 and $CaCl_2$ crosslinkers were applied after the 3D-printing process by immersing the 3D-printed nanocellulose-based hydrogel into the crosslinking solutions. In contrast, ECH was incorporated into the CNF/CMC hydrogel ink formulation prior to the printing process.

This procedure resulted in a minor alteration in the hydrogel's ink for 3D printing. Consequently, the formulation ratio of CNF to CMC had to be adjusted from 4.5% CNF/4.5% CMC to 6% CNF/5% CMC to ensure better printing and shape fidelity. The 3D-printed nanocellulose-based hydrogel was left to dry at room temperature until a

constant weight was observed. For both crosslinkers, a washing process was necessary to eliminate any undesired chemicals before proceeding with the next experiment.

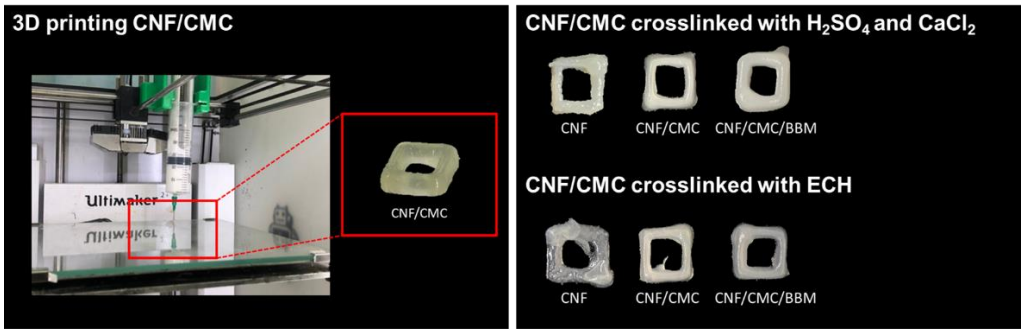

Fig. 2. 3D-printed CNF/CMC hydrogels in square shape for cell adhesion and different types of crosslinking reactions

Microalgae Growth Cells

The microalgal species, *C. vulgaris*, was selected for this study due to its potential health benefits as a dietary supplement, broad range of applications, and adaptable cultivation (Allaguvatova *et al.* 2019; Bito *et al.* 2020). The growth of *C. vulgaris* in BBM was monitored over 20 days by recording the OD and color of the culture media. The growth curve, plotted in Fig. 2(a), was derived from normal cultivation using 10% (v/v) of the initial *C. vulgaris* stock culture. The lag phase was bypassed, and the culture directly entered the log phase due to the suitability of microalgae to adapt in the BBM. The curve has a similar pattern with the sigmoid shape based on the microbial growth, which was predicted based on the Eq. 1 shown below (Beruto *et al.* 2014; Paladino and Neviani 2020),

$$c(t) = c_0 + \frac{k_\alpha}{1+\frac{k_a - c_0}{c_0} exp(-k_1 t)} \quad (1)$$

where c_0 is the initial inoculum concentration (g/L), k_1, is the specific rate constant, and k_a, is a specific rate constant representing the total average probability that cells have to form clusters. The exponential phase lasted approximately 11 days before transitioning to the stationary phase. This indicates that the microalgae actively grew for 11 days, with a remarkable increase in OD reading from 0.2 to 1.2. The stationary phase saw only gradual changes in OD, from 1.2 to 1.5, over the course of nine days since it already achieved zero growth during this period.

The results were further corroborated by the color changes observed in the culture media, as depicted in Fig. 2(b). The initial pale-yellow color on day 0 transitioned to dark green by day 8, a hue that persisted until day 11. From day 12 onwards, the culture media began to display a brownish color, eventually turning completely brown by day 18. This color shift indicates a decline in microalgae cell growth as the green pigment in the cell was disrupted and turned brown. This brown colour also indicates cells that are non-viable due to nutrients deficiency and environmental changes (Ganuza *et al.* 2016; Valdez *et al.* 2018). As shown in Fig. 2(a), during the stationary phase, the *C. vulgaris* cells exhibited a smaller gap in OD readings over several days due to interrupted cell growth. In the subsequent cell adhesion experiment, an OD of 0.7 to 1.2 was maintained, indicating that the *C. vulgaris* was in the exponential phase and exhibited a vibrant green color. Moreover, the capability of microalgae to grow also was explored by the addition of crosslinkers into culture media, as shown in Figs. 2(a,b). The presence of $CaCl_2$ reduced the growth of

microalgal cells, as indicated by lowering the OD value in which it only reached 0.6 on day 10 and gradually decreased afterwards even though the culture media was able to turn green. Meanwhile, the presence of H_2SO_4 and ECH causing the death of microalgae cells on the same day was shown by the decrease in plotted OD value and colour changes in Fig. 3(a,b). The findings from the toxicological study showed that some materials used in the fabrication of hydrogel will interfere and are not suitable for cell growth. The prepared hydrogel needs to undergo a thorough cleaning process before being used in the cell applications.

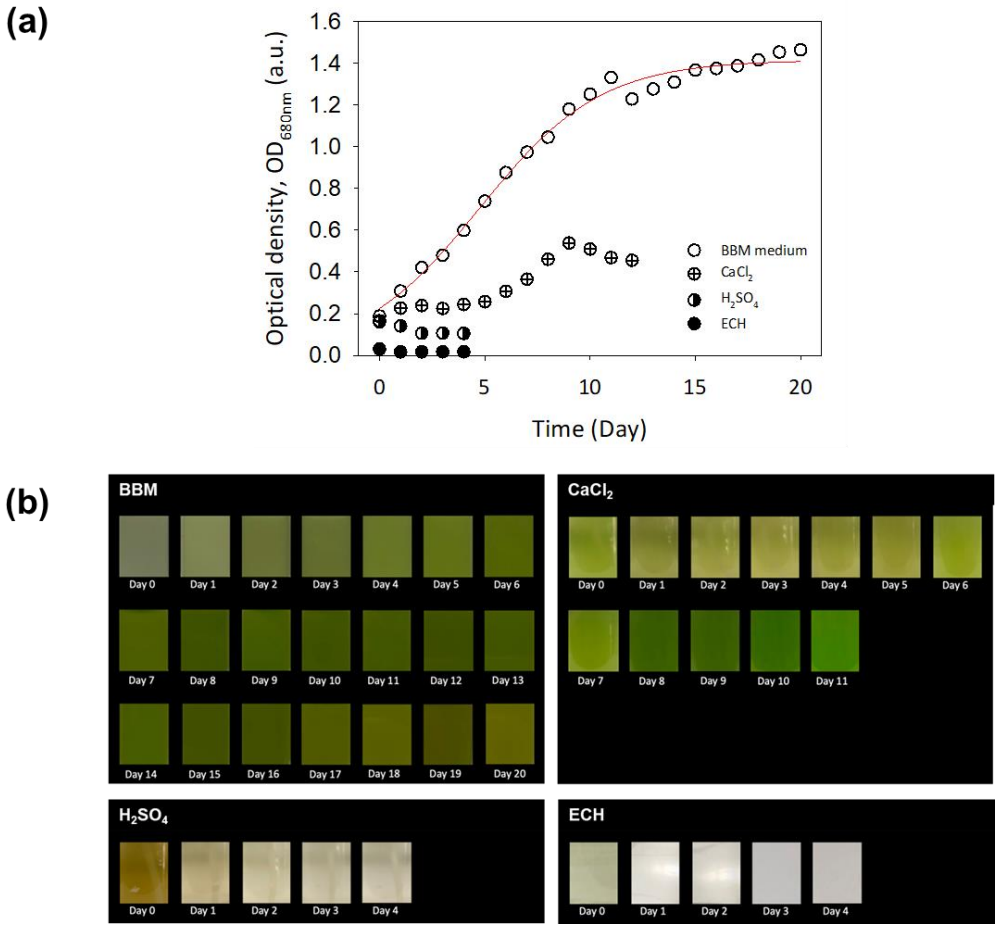

Fig. 3. The observation of (a) optical density and (b) color intensity of the growth of *C. vulgaris* in BBM, $CaCl_2$, H_2SO_4, and ECH for 5 to 20 days

Under the optical microscope, the cellular structure of *C. vulgaris* is spherical, exhibiting a green coloration attributed to the presence of chlorophyll, as depicted in Fig. 3(a). Further analysis using FESEM provided high-resolution micrograph images, offering an intricate view of the *C. vulgaris* cells' surface, as shown in Fig. 3(b). The FESEM images confirmed the preservation of the microalgae cells' morphology, with their characteristic cell shape and size remaining consistent.

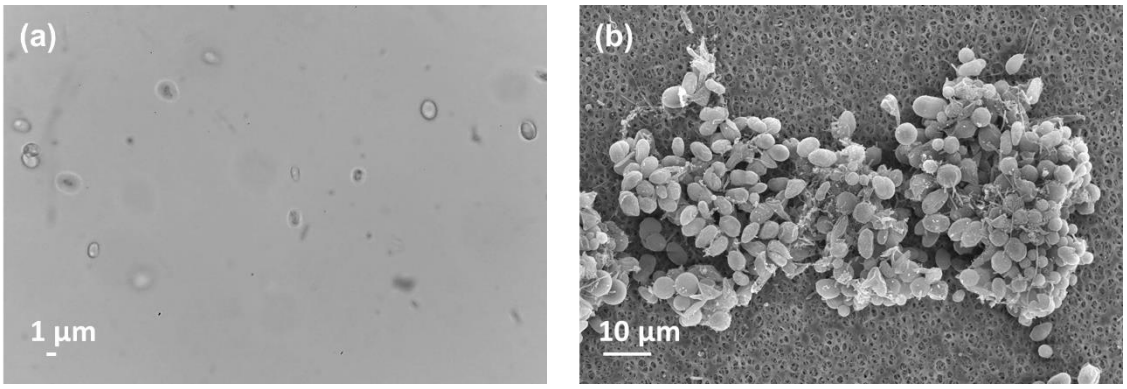

Fig. 4. The (a) optical microscope and (b) micrograph images of *C. vulgaris*

Effect of CNF/CMC Hydrogels in Microalgae Cultivation

Cell attachment refers to the ability of a single cell to adhere to other cells or materials. In this context, the study focuses on the ability of microalgae cells to adhere to cellulose hydrogel. This study helps in understanding the interactions and behavior of cells with biomaterials. The surface of the cellulose hydrogel plays an important role in providing suitable conditions for cell attachment. The 3D-printed cellulose hydrogel, with the presence of two different crosslinker, dual crosslinker (H_2SO_4 and $CaCl_2$) and ECH, was immersed in microalgae culture to study the cell attachment capability.

The growth *of C. vulgaris* at different culture conditions alongside the 3D-printed nanocellulose-based hydrogel was monitored based on OD readings and the color of the hydrogel over an eight-day period. In the study of the impact of CNF/CMC hydrogels, the cultivation was divided into three scopes, each designed to explore different aspects of microalgae growth in relation to CNF/CMC nanocellulose-based hydrogel. The CNF/CMC nanocellulose-based hydrogel was tested for its impact on the growth of microalgae in a fresh culture of *C. vulgaris* (10% of the original culture). Subsequently, the attachment of cells on the hydrogel surface was observed using initial media at exponential phase. *C. vulgaris* is cultivated until it reaches an exponential phase before being transferred and combined with the 3D printed hydrogel across different categories. The encapsulation of cells within the hydrogel matrix was analyzed by injection of 1.0 mL of *C. vulgaris* within the hydrogel to study the cell-hydrogel interactions.

Figures 5(a) and 5(b) display the OD readings of the effect of microalgae growth in the presence of CNF/CMC with different formulations and crosslinkers. By using crosslinkers, H_2SO_4 and $CaCl_2$, (Fig. 5(a)), the readings began to reach 1.0 to 1.2 on day 4 until day 6, which is earlier compared to the normal growth. However, for the ECH crosslinker, the 10% stock culture directly increased at the early stage of cultivation with the reading of 0.1 - 1.0 (Fig. 5(b)). The growth rate was observed to increase more rapidly compared to H_2SO_4 and $CaCl_2$ especially for CNF-2. However the OD readings of CNF/CMC-2 and CNF/CMC/BBM-2 hydrogels only showed an increase up to 0.8, possibly due to incomplete washing process of hydrogel. The hydrogel acts as a scaffold and facilitates the initial cell attachment during the culture process, which resulted in a significant increase in growth rate (Salehi *et al.* 2024). Increases in the cell growth rate cause growth limiting factors to occur earlier especially in terms of nutrient sources. This also contributes to the faster transition from exponential phase to the stationary phase.

Figure 5(c) presents the physical appearance of the 3D-printed nanocellulose-based hydrogel after cultivation. This was indicated by the greenish color on the biomaterial

surface, which signifies the presence of microalgal cells. Cell attachment on the CNF/CMC hydrogel was more pronounced with the use of dual crosslinking, H_2SO_4 and $CaCl_2$, compared to ECH. The presence of green colour on the hydrogel surface could be clearly observed, especially for CNF/CMC-1 and CNF/CMC/BBM-1. In the case of the different hydrogel crosslinkers, although ECH crosslinker produced a more rigid 3D-printed nanocellulose-based hydrogel, it also prevented the microalgae from attaching to the surface, as shown by the lack of color changes. Only a small green spot of microalgae is visible at the fracture point of the hydrogel. This suggests that the microalgal cell adhesion on the CNF/CMC hydrogel was more pronounced in the presence of H_2SO_4 and $CaCl_2$ than ECH and could be related to the surface condition of the hydrogel. From the literature it is stated that materials with hydrophobic properties and high surface roughness tend to attract cells for attachment (Chang and Wang 2011; Ferrari *et al.* 2019; Majhy *et al.* 2021). This may explain why H_2SO_4 or $CaCl_2$ as crosslinker produced the hydrogel with higher surface roughness and hydrophobicity than ECH. However, the surface characteristic has not yet been analyzed. From the collected images, the results clearly show that the new culture medium aids in cell attachment. A higher intensity of green color can be clearly observed, especially in the CNF/CMC hydrogel with H_2SO_4 and $CaCl_2$, dual crosslinking.

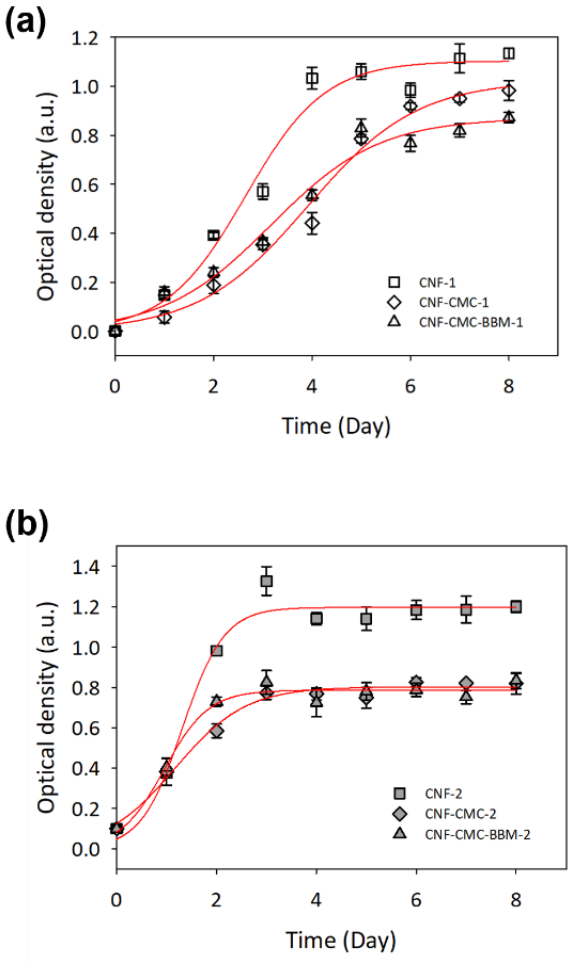

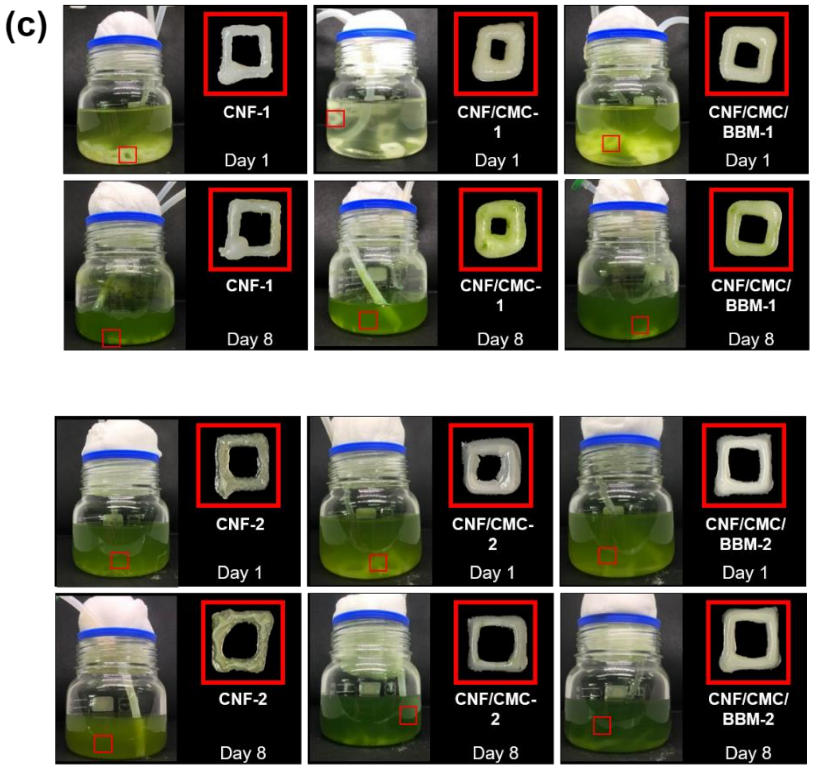

Fig. 5. The optical density of the new culture media for 8 days with different hydrogels crosslinker of (a) H_2SO_4 and $CaCl_2$, (b) ECH crosslinking and (c) physical appearance of 3D printed nanocellulose-based hydrogel

Microalgal Cell Adhesion on CNF/CMC Hydrogels

In this context, the study focuses on the capability of microalgal cells to attach to a nanocellulose-based hydrogel. This experiment aids in understanding the interaction and behavior of the cells with the biomaterial. Figures 6(a) and 6(b) present the cell attachment impacts on the hydrogels in the exponential phase culture medium. The optical density was maintained between 0.7 to 1.2 as the *C. vulgaris* is in the active phase and showed a deep green colour. As shown in Fig. 6(a,b), the OD reading declines in the early 3 days before it started to increase, possibly because the microalgae cells adaptation with the new environment in the presence of hydrogel. However, cells reactivated after the adaptation period in which early 3 days. This phenomenon may indicate an attachment interaction between the microalgae and the substrate. The surface of the nanocellulose-based hydrogel played a crucial role in providing suitable conditions for cell binding.

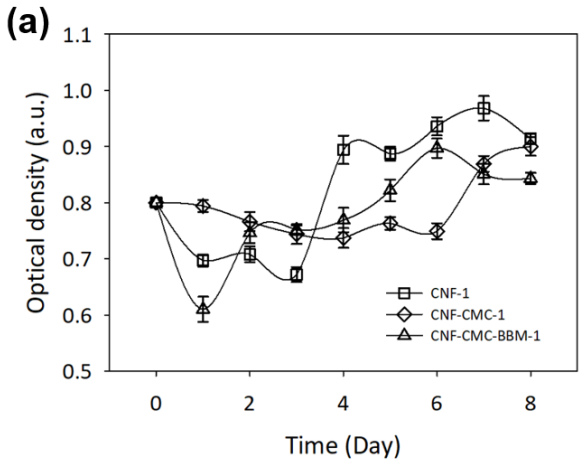
(a)
Optical density (a.u.)
1.1
1.0
0.9
0.8
0.7
0.6
0.5
0
2
4
6
8
Time (Day)
CNF-1
CNF-CMC-1
CNF-CMC-BBM-1

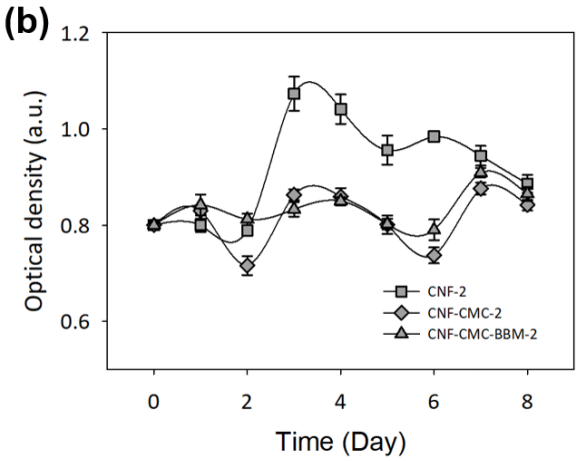
(b)
Optical density (a.u.)
1.2
1.0
0.8
0.6
0
2
4
6
8
Time (Day)
CNF-2
CNF-CMC-2
CNF-CMC-BBM-2

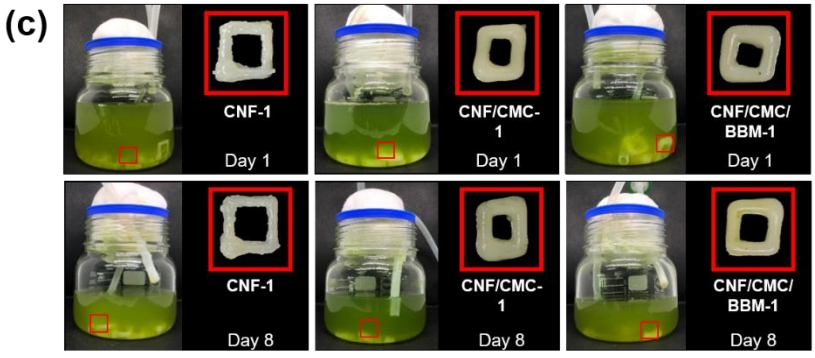
(c)
CNF-1
Day 1
CNF/CMC-1
Day 1
CNF/CMC/BBM-1
Day 1
CNF-1
Day 8
CNF/CMC-1
Day 8
CNF/CMC/BBM-1
Day 8

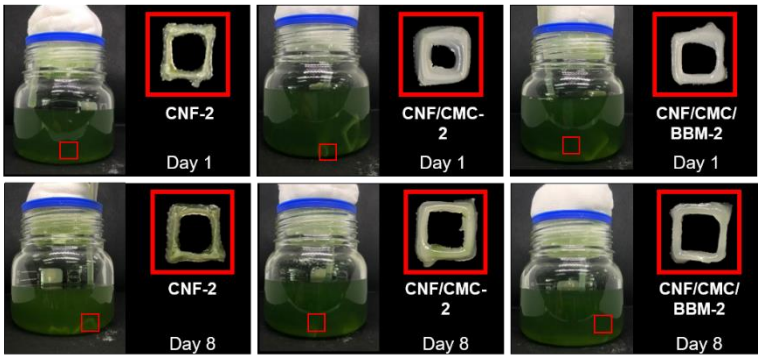

Fig. 6. The optical density of the exponential phase culture media for 8 days with different hydrogels crosslinker of (a) H_2SO_4 and $CaCl_2$, (b) ECH crosslinking and (c) physical appearance of 3D printed nanocellulose-based hydrogel

Moreover, adhesion of *C. vulgaris* was observed in this study based on the color of the hydrogel after being immersed in culture media (see Fig. 6(c)). However, culture media in exponential phase exhibited minimal to no color alteration from day 1 to day 6. Notably, the new culture conditions of CNF/CMC and CNF/CMC/BBM (Fig. 4) exhibited a higher color intensity. The adherence of *C. vulgaris* escalated with the cell growth in the culture medium. As the cells proliferated, they sought out available surfaces to latch onto, facilitating their growth. However, when cell growth was consistent and the OD remained in the exponential phase, cell adhesion became less preferred, as optimal growth had been attained and cell division began to wane. As depicted in Fig. 6(c), *C. vulgaris* cells demonstrated a preference for the CNF/CMC hydrogel over CNF alone. These experimental findings were supported by some previous study on the high potential of microalgal cell attachment using different biomaterial, as summarized in Table 2.

Table 2. The Capability of Cell Attachment on Different Substrate Material and Microalgae Species

Material	Algae Species	Cultivation Method	Attachment Capability	References
Cotton and jute	Microalgae (*Scenedesmus vacuolatus* ACUF 053)	Batch system	80% attachment on cotton in 4 days	Carbone *et al.* 2017
Biofilm membrane	*Chlorella vulgaris*	Photobioreactor	72.4% immobilized on biofilm	Gao *et al.* 2014
Polyacrylamide hydrogels	*Chlorella vulgaris*	Batch system	Increase the biomass production due to high attachment	González-Delgado *et al.* 2016
Polyethylenimine-based sorbents	*Chlorella vulgaris*	Batch system	> 80% P-ECH in 24 h and cell vigorously attaches during stationary phase	Vasilieva *et al.* 2018

The image analysis of microalgal cell attachment on 3D-printed CNF/CMC hydrogel was performed by using ImageJ software as shown in Fig. 7. The attachment of microalgal cells on the 3D-printed biomaterial surfaces can be visualized by isolating and analyzing the green channels within the image data, which reveal the presence of the characteristic green pigments found in microalgae. These pigments, typically chlorophyll, are indicative of microalgal cells, and their detection through the split green channels serves as a confirmation of cell attachment on the biomaterial substrate. Previous studies have mentioned the changes of thin yellow layer to green layer as the growth of cells corresponds to the area of cells coverage generated by imaging data (Berner *et al.* 2015; Carbone *et al.* 2017). Whiter color observed on the CNF/CMC/BBM-1 formulation compared to CNF/CMC-1 which explains that the presence of BBM in the biomaterial formulation promotes the cell adherences on the hydrogel surface.

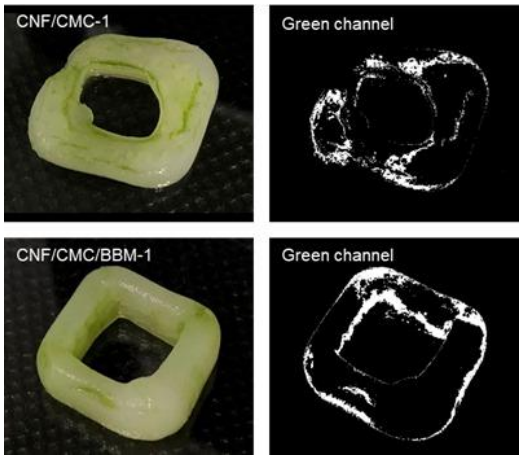

Fig. 7. The image analysis of microalgal cell attachment on 3D-printed CNF/CMC hydrogel

Encapsulation Microalgae Cell in CNF/CMC Hydrogels

Figure 8(a) illustrates the growth of encapsulated microalgae in the 3D-printed nanocellulose-based hydrogel. The CNF/CMC hydrogel encapsulated with microalgae had been cultivated in BBM media for 8 days. Initially, from day 0 to day 3, a lag phase was observed, characterized by an absence of microalgae growth within the BBM media. However, expansion of *C. vulgaris* from the hydrogel to the BBM media occurred on day 3, prompting the cells to grow and enter the exponential phase.

Encapsulation of *C. vulgaris* into the hydrogel exhibited the most noticeable color transformation from white to green, as shown in Fig. 8(b). The gradual change is likely attributable to the prolonged lag phase followed by an extended period of exponential growth experienced by the microalgae. As the *C. vulgaris cells* adapted to the hydrogel environment, they exhibited an increased period of attachment, which was conducive to cell division by gradually turning the hydrogel to green colour. In line with previous observations, the hydrogel's green coloration was more pronounced when the hydrogel was crosslinked with H_2SO_4 and $CaCl_2$, compared to ECH. This suggests that the chemical composition of the hydrogel plays a significant role in the microalgae's presence and growth. Decreases in cell attachment can be related to the surface characteristic of hydrogel since the OD reading of culture medium showed almost similar trend for both types of crosslinker.

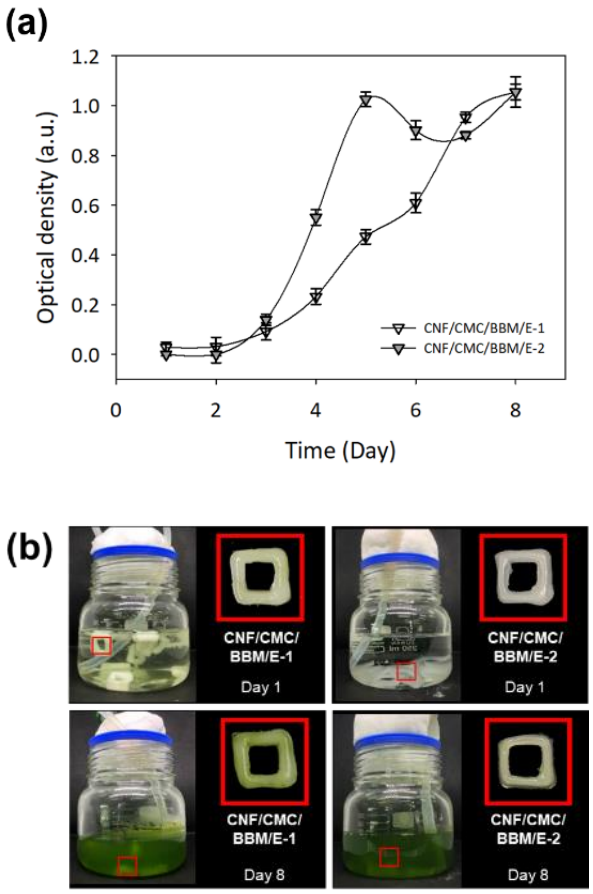

Fig. 8. The optical density of the encapsulated culture media for 8 days with different hydrogels crosslinker of (a) H_2SO_4 and $CaCl_2$ and ECH crosslinking and (b) physical appearance of 3D printed nanocellulose-based hydrogel

CONCLUSIONS

Cellulose-based hydrogels, especially those containing CNF and CMC, show promise for various applications, including biomedical and cell culturing. This works was conducted to analyze the potential of these hydrogels for 3D printing and their interaction with living cells.

1. The viscosity of the ink was found to play a crucial role in achieving a well-defined printed shape. The CNF/CMC hydrogel, when crosslinked with two types of crosslinkers, achieved excellent performance for 3D printing, particularly in liquid deposition modeling. Adjusting the CNF to CMC ratio may be necessary after adding the crosslinker to achieve optimal results.
2. In terms of cell growth, the growth of *C. vulgaris* cells in BBM solution exhibited similar trends for both the standard culture and the culture media incorporating the CNF/CMC hydrogels. It was found that the use of H_2SO_4 and $CaCl_2$ in hydrogel formation was more conducive to cell attachment compared to using epichlorohydrin. Besides, longer lag phase would contribute to higher cell attachment, as shown by the new culture and encapsulation experiment.

ACKNOWLEDGMENTS

The authors are grateful for the support of the Universiti Kebangsaan Malaysia, Grant No. DIP-2023-002.

REFERENCES CITED

Allaguvatova, R., Myasina, Y., Zakharenko, V., and Gaysina, L. (2019). "A simple method for the cultivation of algae *Chlorella vulgaris* Bejerinck," *IOP Conference Series: Earth and Environmental Science* 390, 1-5. DOI: 10.1088/1755-1315/390/1/012020

Annabi, M., Nichol, J. W., Zhong, X., Ji, C., Koshy, S., Khademhosseini, A., and Dehghani, F. (2010). "Controlling the porosity and microarchitecture of hydrogels for tissue engineering," *Tissue Eng Part B Rev* 16(4), 371-383. DOI: 10.1089/ten.teb.2009.0639

Anderson, R. A. (2005). *Algae Culturing Techniques*, Elsevier Academic Press, Cambridge, MA, USA.

Ban, M. T., Mahadin, N., and Abd Karim, K. J. (2022). "Synthesis of hydrogel from sugarcane bagasse extracted cellulose for swelling properties study," *Materials Today: Proceedings* 50(3), 2567-2575. DOI: 10.1016/j.matpr.2021.08.342

Bar-Shai, N., Sharabani-Yosef, O., Zollmann, M., Lesman, A., and Golberg, A. (2021). "Seaweed cellulose scaffolds derived from green macroalgae for tissue engineering," *Scientific Reports* 11(1), 1–17. DOI: 10.1038/s41598-021-90903-2

Berner, F., Heimann, K., and Sheehan, M. (2014). "Microalgal biofilms for biomass production," *Journal of Applied Phycology* 27(5), 1793-1804. DOI: 10.1007/s10811-014-0489-x

Beruto, D. T., Lagazzo, A., Frumento, D., and Converti, A. (2014). "Kinetic model of *Chlorella vulgaris* growth with and without extremely low frequency-electromagnetic fields (EM-ELF)," *Journal of Biotechnology* 169(1), 9-14. DOI: 10.1016/j.jbiotec.2013.10.035

Bito, T., Okumura, E., Fujishima, M., and Watanabe, F. (2020). "Potential of *Chlorella* as a dietary supplement to promote human health," *Nutrients* 12(9), article 2524. DOI: 10.3390/nu12092524

Carbone, D. A., Gargano, I., Pinto, G., De Natale, A., and Pollio, A. (2017). "Evaluating microalgae attachment to surfaces: A first approach towards a laboratory integrated assessment," *Chemical Engineering Transactions* 57, 73-78. DOI: 10.3303/CET1757013

Chang, H. -I., and Wang, Y. (2011). "Cell responses to surface and architecture of tissue engineering scaffolds," In: *Regenerative Medicine and Tissue Engineering - Cells and Biomaterials*, IntechOpen, London, UK. DOI: 10.5772/21983

Chen, C., Xi, Y., and Weng, Y. (2022). "Recent advances in cellulose-based hydrogels for tissue engineering applications," *Polymers* 14(16), article 3335. DOI: 10.3390/polym14163335

Chopra, L., and Manikanika. (2022). "Extraction of cellulosic fibers from the natural resources: A short review," *Materials Today: Proceedings* 48(17), 1265-1270. DOI: 10.1016/j.matpr.2021.08.267

Ciolacu, D. E., Nicu, R., and Ciolacu, F. (2020). "Cellulose-based hydrogels as sustained drug-delivery systems," *Materials* 13(22), article 5270. DOI: 10.3390/ma13225270

Correa, S., Grosskopf, A. K., Hernandez, H. L., Chan, D., Yu, A. C., Stapleton, L. M., and Appel, E. A. (2021). "Translational applications of hydrogels," *Chemical Reviews* 121(18), 11385-11457. DOI: 10.1021/acs.chemrev.0c01177

Cui, X., Lee, J. J. L., and Chen, W. N. (2019). "Eco-friendly and biodegradable cellulose hydrogels produced from low cost okara: Towards non-toxic flexible electronics," *Scientific Reports* 9(1), 1-9. DOI: 10.1038/s41598-019-54638-5

Dattilo, M., Patitucci, F., Prete, S., Parisi, O. I., and Puoci, F. (2023). "Polysaccharide-based hydrogels and their application as drug delivery systems in cancer treatment: A review," *Journal of Functional Biomaterials* 14(2), article 55. DOI: 10.3390/jfb14020055

Ferrari, M., Cirisano, F., and Morán, C. M. (2019). "Mammalian cell behavior on hydrophobic substrates: Influence of surface properties," *Colloids and Interfaces* 3(2), article 48. DOI: 10.3390/colloids3020048

Ganuza, E., Sellers, C. E., Bennett, B. W., Lyons, E. M., and Carney, L. T. (2016). "A novel treatment protects *Chlorella* at commercial scale from the predatory bacterium *Vampirovibrio chlorellavorus*," *Frontiers in Microbiology* 7, 1-13. DOI: 10.3389/fmicb.2016.00848

Gao, F., Yang, Z. -H., Li, C., Zeng, G. -M., Ma, D. -H. and Zhou, L. (2015). "A novel algal biofilm membrane photobioreactor for attached microalgae growth and nutrients removal from secondary effluent," *Bioresource Technology* 179, 8-12. DOI: 10.1016/j.biortech.2014.11.108

González-Díaz, E. C., and Varghese, S. (2016). "Hydrogels as extracellular matrix analogs," *Gels* 2(3), article 20. DOI: 10.3390/gels2030020

González-Delgado, Á. D., Barajas-Solano, A. F., and Peralta-Ruiz, Y. Y. (2016). "Microalgae immobilization using hydrogels for environmental applications: Study of transient photopolymerization," *Chemical Engineering Transactions* 47, 457-462. DOI: 10.3303/CET1647077

Griffiths, M. J., Garcin, C., van Hille, R. P., and Harrison, S. T. (2011). "Interference by pigment in the estimation of microalgal biomass concentration by optical density," *Journal of Microbiological Methods* 85(2), 119-123. DOI: 10.1016/j.mimet.2011.02.005

Hua, Y. L., Harun, S., Sajab, M. S., Jahim, J. M., and Shah, S. S. M. (2020). "Extraction of cellulose and microcrystalline cellulose from kenaf," *Jurnal Kejuruteraan* 32(2), 205-213. DOI: 10.17576/jkukm-2020-32(2)-04

Johns, M. A., Bae, Y., Guimaraes, F. E. G., Lanzoni, E. M., Costa, C. A. R., Murray, P. M., Deneke, C., Galembeck, F., Scott, J. L., and Sharma, R. I. (2018). "Predicting ligand-free cell attachment on next-generation cellulose-chitosan hydrogels," *ACS Omega* 3(1), 937-945. DOI: 10.1021/acsomega.7b01583

Jusoh, W. N. L. W., Sajab, M. S., Abdul, P. M., and Kaco, H. (2022). "Recent advances in 3D bioprinting: A review of cellulose-based biomaterials ink," *Polymers* 14(11), article 2260. DOI: 10.3390/polym14112260

Jusoh, W. N. L. W., Mohan, D., Sajab, M. S., Abdul, P. M., Kaco, H., Ding, G. and Baini, R. (2023). "Nanocellulose-based biomaterial ink hydrogel for uptake/release of bovine serum albumin," *Polymers* 15(4), article 837. DOI: 10.3390/polym15040837

Kabir, S. M. F., Sikdar, P. P., Haque, B., Bhuiyan, M. A. R., Ali, A., and Islam, M. N. (2018). "Cellulose-based hydrogel materials: Chemistry, properties and their prospective applications," *Progress in Biomaterials* 7(3), 153-174. DOI: 10.1007/s40204-018-0095-0

Kargarzadeh, H., Huang, J., Lin, N., Ahmad, I., Mariano, M., Dufresne, A., Thomas, S., and Gałęski, A. (2018). "Recent developments in nanocellulose-based biodegradable polymers, thermoplastic polymers, and porous nanocomposites," *Progress in Polymer Science* 87, 197-227. DOI: 10.1016/j.progpolymsci.2018.07.008

Langer, R. (2000). "Biomaterials in drug delivery and tissue engineering: One laboratory's experience," *Accounts of Chemical Research* 33(2), 94-101. DOI: 10.1021/ar9800993

Liu, A. P., Appel, E. A., Ashby, P. D., Baker, B. M., Franco, E., Gu, L., Haynes, K., Joshi, N. S., Kloxin, A. M., Kouwer, P. H. J., *et al*. (2022). "The living interface between synthetic biology and biomaterial design," *Nature Materials* 21(4), 390–397. DOI: 10.1038/s41563-022-01231-3

Liu, S., Yu, J. -M., Gan, Y. -C., Qiu, X. -Z., Gao, Z. -C., Wang, H., Chen, S. -X., Xiong, Y., Liu, G. -H., Lin, S. -E., *et al*. (2023). "Biomimetic natural biomaterials for tissue engineering and regenerative medicine: New biosynthesis methods, recent advances, and emerging applications," *Military Medical Research* 10(1), 1-30. DOI: 10.1186/s40779-023-00448-w

Loh, E. Y. X., Mohamad, N., Fauzi, M. B., Ng, M. H., Ng, S. F., and Mohd Amin, M. C. I. (2018). "Development of a bacterial cellulose-based hydrogel cell carrier containing keratinocytes and fibroblasts for full-thickness wound healing," *Scientific Reports* 8(1), 1-12. DOI: 10.1038/s41598-018-21174-7

Majhy, B., Priyadarshini, P., and Sen, A. K. (2021). "Effect of surface energy and roughness on cell adhesion and growth-facile surface modification for enhanced cell culture," *RSC Advances* 11(25), 15467-15476. DOI: 10.1039/d1ra02402g

Mantha, S., Pillai, S., Khayambashi, P., Upadhyay, A., Zhang, Y., Tao, O., Pham, H. M., and Tran, S. D. (2019). "Smart hydrogels in tissue engineering and regenerative medicine," *Materials* 12(20), article 3323. DOI: 10.3390/ma12203323

Mohan, D., Teong, Z. K., Sajab, M. S., Kamarudin, N. H. N., and Kaco, H. (2021). "Intact fibrillated 3D-printed cellulose macrofibrils/$CaCO_3$ for controlled drug delivery," *Polymers* 13(12), article 1912. DOI: 10.3390/polym13121912

Naomi, R., Idrus, R. B. H., and Fauzi, M. B. (2020). "Plant- *vs*. bacterial-derived cellulose for wound healing: A review," *International Journal of Environmental Research and Public Health* 17(18), article 6803. DOI: 10.3390/ijerph17186803

Norioka, C., Inamoto, Y., Hajime, C., Kawamura, A., and Miyata, T. (2021). "A universal method to easily design tough and stretchable hydrogels," *NPG Asia Materials* 13(1), 1–10. DOI: 10.1038/s41427-021-00302-2

Pajorova, J., Skogberg, A., Hadraba, D., Broz, A., Travnickova, M., Zikmundova, M., Honkanen, M., Hannula, M., Lahtinen, P., Tomkova, M., *et al*. (2020). "Cellulose mesh with charged nanocellulose coatings as a promising carrier of skin and stem cells for regenerative applications," *Biomacromolecules* 21(12), 4857-4870. DOI: 10.1021/acs.biomac.0c01097

Paladino, O., and Neviani, M. (2020). "Scale-up of photo-bioreactors for microalgae cultivation by π-theorem," *Biochemical Engineering Journal* 153, article ID 107398. DOI: 10.1016/j.bej.2019.107398

Pyarasani, R. D., Jayaramudu, T., and John, A. (2018). "Polyaniline-based conducting hydrogels," *Journal of Materials Science* 54(2), 1-23. DOI: 10.1007/s10853-018-2977-x

Sajab, M. S., Mohan, D., Santanaraj, J., Chia, C. H., Kaco, H., Harun, S., and Kamarudin, N. H. N. (2019). "Telescopic synthesis of cellulose nanofibrils with a stable dispersion of Fe(0) nanoparticles for synergistic removal of 5-fluorouracil," *Scientific Reports* 9(1), 1–11. DOI: 10.1038/s41598-019-48274-2

Salehi, B., Zhang, B., Nowlin, K., Wang, L., and Shahbazi, A. (2024). "A multifunctional cellulose- and starch-based composite hydrogel with iron-modified biochar particles for enhancing microalgae growth," *Carbohydrate Polymers* 327, article ID 121657. DOI: 10.1016/j.carbpol.2023.121657

Scarponi, P., Ghirardini, A. V., Bravi, M., and Cavinato, C. (2021). "Evaluation of *Chlorella vulgaris* and *Scenedesmus obliquus* growth on pretreated organic solid waste digestate," *Waste Management* 119, 235-241. DOI: 10.1002/sapm1966451109

Tan, M. S. F., White, A. P., Rahman, S., and Dykes, G. A. (2016). "Role of fimbriae, flagella and cellulose on the attachment of *Salmonella* Typhimurium ATCC 14028 to plant cell wall models," *PLoS ONE* 11(6), article ID 0158311. DOI: 10.1371/journal.pone.0158311

Troy, E., Tilbury, M. A., Power, A. M., and Wall, J. G. (2021). "Nature-based biomaterials and their application in biomedicine," *Polymers* 13(19), article 3321. DOI: 10.3390/polym13193321

Valdez, C., Perengüez, Y., Mátyás, B., and Guevara, M. F. (2018). "Analysis of removal of cadmium by action of immobilized *Chlorella* sp. micro-algae in alginate beads," *F1000Research* 7(54), 1-7. DOI: 10.12688/f1000research.13527.1

Vasilieva, S., Shibzukhova, K., Morozov, A., Solovchenko, A., Bessonov, I., Kopitsyna, M., Lukyanov, A., Chekanov, K., and Lobakova, E. (2018). "Immobilization of microalgae on the surface of new cross-linked polyethylenimine-based sorbents," *Journal of Biotechnology* 281, 31-38. DOI: 10.1016/j.jbiotec.2018.03.011

Vel, R., Bhatt, A., Priyanka, A., Gauthaman, A., Anilkumar, V., Safeena, A. S., and Ranjith, S. (2022). "DEAE- Cellulose-based composite hydrogel for 3D printing application: Physicochemical, mechanical, and biological optimization," *Materials Today Communications* 33, article ID 104335. DOI: 10.1016/j.mtcomm.2022.104335

Yap, J. X., Leo, C. P., Chan, D. J. C., Yasin, N. H. M., and Sajab, M. S. (2023). "*Chlorella vulgaris* nanocellulose in hydrogel beads for dye removal," *Separation and Purification Technology* 324, article ID 124613. DOI: 10.1016/j.seppur.2023.124613

Zainal, S. H., Mohd, N. H., Suhaili, N., Anuar, F. H., Lazim, A. M., and Othaman, R. (2021). "Preparation of cellulose-based hydrogel: A review," *Journal of Materials Research and Technology* 10(6), 935-952. DOI: 10.1016/j.jmrt.2020.12.012

Zou, P., Yao, J., Cui, Y. -N., Zhao, T., Che, J., Yang, M., Li, Z., and Gao, C. (2022). "Advances in Cellulose-based hydrogels for biomedical engineering: A review summary," *Gels* 8(6), article 364. DOI: 10.3390/gels8060364

Article submitted: May 16, 2024; Peer review completed: June 20, 2024; Revised version received: August 7, 2024; Accepted: October 29, 2024; Published: November 11, 2024.
DOI: 10.15376/biores.20.1.201-218